# Study of neutron beam divergence in a beam-fusion scenario employing laser driven ions

A. Alejo[a], S. Kar[a,*], A. Green[a], H. Ahmed[a], A.P.L. Robinson[b], M. Cerchez[c], R. Clarke[b], D. Doria[a], S. Dorkings[b], J. Fernandez[b], P. McKenna[d], S.R. Mirfayzi[a], K. Naughton[a], D. Neely[b], P. Norreys[b,1], C. Peth[c], H. Powell[d], J.A. Ruiz[e], J. Swain[f], O. Willi[c], M. Borghesi[a]

[a]*Centre for Plasma Physics, School of Mathematics and Physics, Queen's University Belfast, BT7 1NN, UK*
[b]*Central Laser Facility, Rutherford Appleton Laboratory, Didcot, Oxfordshire, OX11 0QX, UK*
[c]*Institut für Laser-und Plasmaphysik, Heinrich-Heine-Universität, Düsseldorf, Germany*
[d]*Department of Physics, SUPA, University of Strathclyde, Glasgow G4 0NG*
[e]*Colegio Los Naranjos, Fuenlabrada, 28941, Madrid, Spain*
[f]*Rudolf Peierls Centre for Theoretical Physics, University of Oxford, Oxford, OX1 3NP, UK*

**Abstract**

The most established route to create a laser based neutron source is by employing laser accelerated low atomic number ions in fusion reactions. In addition to benefiting from the high reaction cross-sections at moderate energy of projectile ions, affordable using the currently available lasers, anisotropy in the neutron emission is another facet of beam-fusion reactions. Using a simple numerical model based on neutron generation in a pitcher-catcher scenario, anisotropy in neutron emission was studied for the deuterium-deuterium fusion reaction. Simulation results are in good agreement with the narrow-divergence ($\sim 70^\circ$ full width at half maximum) neutron beam recently obtained from an experiment (reported in Kar *et al.*, arXiv:1507.04511). By varying the input ion beam parameters, simulations show a further improvement in the neutron beam directionality (i.e. reduction in beam divergence) with the increase in the projectile ion beam temperature and cut-off energy, expected from the interactions of higher laser intensities at upcoming facilities.

*Keywords:* laser, neutron, beam fusion

## 1. Introduction

Fast neutron sources driven by high-power lasers have gained substantial interest over the last decades for a range of potential applications in medicine [1], security [2, 3], material science [4] and high energy density physics research [5]. Furthermore, deploying compact moderators closely coupled to laser-driven fast neutrons sources would allow development of intense sources of thermal and epithermal neutrons, which would extend the range of applicability of the source. With the rapid progress in laser technology, aiming towards developing higher repetition rate lasers of higher powers, laser-driven neutron sources can, in principle, complement the research activities currently pursued at conventional accelerator-driven spallation sources. Although large scale facilities produces substantially higher fast neutron flux, a key interest for laser-driven neutron sources lies in the neutron burst duration, which is substantially shorter than that produced at spallation facilities.

With the current laser systems, neutron yields in excess of $10^{10}$ neutrons/shot have been shown experimentally ([6] and references therein), by employing laser driven ions to generate neutrons from secondary catcher targets via beam-fusion reaction. In addition to the advantage of the ultra-short pulse duration, directionality/anisotropicity in neutron emission is another important characteristic of the beam-fusion reaction. The total neutron yield from a fusion reaction scales with the product of fusing ion densities and cross-section $\sigma$, which, for the most common reactions, reaches high values for centre-of-mass energy in the MeV-10s of MeV range [7]. In a pitcher-catcher scenario, where neutrons are produced by bombarding the laser-driven ions on a suitable converter target, anisotropy arises

*Corresponding author.
Email address: s.kar@qub.ac.uk

from the nuclear reaction kinematics, which strongly depend on the atomic mass of the fusing nuclei and velocity of the projectile ions [6]. In addition, strong angular dependence of the differential cross-section for light nuclei reactions helps producing neutron flux strongly peaked along the incident ion-beam direction, even while using moderate energy (10s of MeV) ions affordable by currently available laser intensities [8]. Therefore, fusion reactions based on low atomic mass nuclei, such as $^{7}$Li(p,n)$^{7}$Be, $^{9}$Be(p,n)$^{9}$B, $^{13}$C(p,n)$^{13}$N, d(d,n)$^{3}$He, T(d,n)$^{4}$He, $^{7}$Li(d,xn), $^{7}$Be(d,xn), etc., are particularly relevant, which would not only allow obtaining higher neutron yield, but higher peak flux by producing a narrow cone beam of neutrons. A highly beamed neutron flux would be extremely helpful towards improving transport capabilities as well as efficient moderation of the neutrons to thermal and epithermal energies by using compact, closely-coupled, directional moderators.

Anisotropic emission of the neutron beam is starting to be realized in experiments. In addition to the anisotropicity intrinsic to the beam-fusion, as discussed above, the neutron beam divergence from a typical laser-driven pitcher-catcher source also depends strongly on the divergence of the projectile ions the final neutron beam divergence from the catcher will be a convolution of the divergence of the input ion beam and the neutron beam divergence expected for a collimated beam of ions. Therefore we developed a simple model to simulate neutron generation from light nuclei reactions in a pitcher-catcher scenario and to study the effect of ion beam parameters (divergence and spectrum) on neutron generation. In this paper we show the beamed neutron emission from d(d,n)$^{3}$He while using laser-driven deuterium beam produced by the target normal sheath acceleration (TNSA) mechanism[8], which compares well with the data obtained from a recent experiment (reported in [6]). A systematic study by varying the input ion beam parameters show that the neutron beam divergence strongly depend on the input ion energy and divergence, which, in principle, can be reduced down to few tens of degree full cone divergence with the TNSA ion beams expected from higher intensity lasers at upcoming facilities[9, 10].

## 2. Simulation design and method

Alternative to the usual Monte-Carlo approach [11, 12] to simulate neutron generation in a beam-fusion scenario, our model takes advantage of the tabulated angularly-resolved neutron yield, that can be found in the literature, obtained for a mono-energetic, pencil beam of ions impinging a catcher at normal incidence. The main interaction that is taken into account in our simple model is the effect of a multi-energy, divergent beam of ions, for instance that typically produced by the TNSA mechanism, towards the angular distribution of emitted neutrons from a secondary catcher target. The schematic of the setup used in our model is shown in Fig. 1.

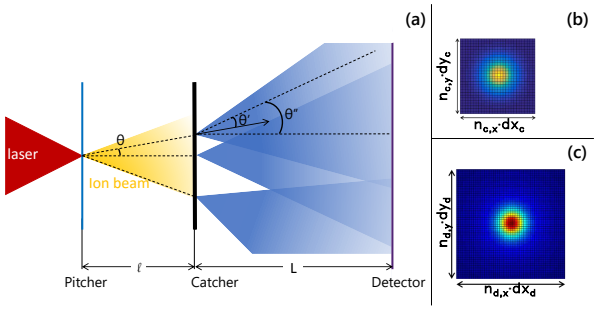


Figure 1: **(a)** Schematic of the neutron generation process in the pitcher-catcher scheme. An ion beam is generated by the interaction of the laser with the target (pitcher), which then reaches the secondary converter (catcher), leading to the neutron emission. **(b)** and **(c)** depict the grids representing the catcher and the detector, respectively.

The input for the projectile ion beam in our model is the angularly-resolved ion spectra. This information can either be obtained numerically, by performing multi-dimensional PIC simulations of the laser-foil interaction, or experimentally, by using for example angularly distributed high-resolution Thomson Parabola Spectrometers (TPS) [13]. The angularly resolved ion spectra can be represented by a function $\frac{d^2N_{ion}}{dE\,d\Omega}(E,\theta,\varphi)$, where $E$ is the ion energy, $(\theta,\varphi)$ are the angles defining the direction of a given beamlet of ion, and $\Omega$ stands for solid angle. For simplicity, one may assume the ion beam produced by the laser-foil interaction to be cylindrically symmetrical about $\theta$.

The catcher in the model was designed as a two dimensional matrix ($n_{c,x} \times n_{c,y}$ cells), where the grid size ($dx_c \times dy_c$) can be chosen depending on the desired resolution and accuracy, being $dx_c = dy_c = 200\,\mu$m the resolution for the simulations here shown. The spectrum of ions arriving at each grid point on the catcher ($dN_{ion,(x,y)}/dE$) is calculated from the input ion spectrum to the code (as mentioned above) for a given pitcher-to-catcher distance ($l$). In order to obtain the neutron flux distribution across a plane parallel to the catcher, the detector in the code was modelled as a two dimensional array of $n_{d,x} \times n_{d,y}$ cells of size $dx_d \times dy_d$. This detector configuration mimics the response of CR39 nuclear track detectors typically used in neutron generation ex-

periments [6, 14, 15], allowing for a direct comparison between the simulations and the experimental data.

Neutron generation from each grid point of the catcher was calculated by using the tabulated data for the angularly-resolved neutron yield, that can either be found in the literature, or be obtained by running Monte Carlo simulations [11, 12] for different ion energies. In this paper we used the tabulated data for d(d,n)$^3$He reaction provided by Davis *et al.*[12], which was one of the main reactions producing neutron in our experiment (reported in [6]). The d(d,n)$^3$He reaction is also an efficient fusion reaction for moderate-energy deuterons, which is suitable for studying the effect of the input ion beam spectrum and divergence on the neutron beam divergence. The tabulated neutron yield per incident ion, given in Ref. [12], along different angles of neutron emission and for different projectile ion energies were interpolated to obtain a function $Y_n(E, \theta')$, where $\theta'$ is the neutron emission angle with respect to the incident ion beam. Using this function, the neutron flux at a given pixel of the detector ($F_{n,(x_d,y_d)} = N_{n,(x_d,y_d)}/dx_d dy_d$) is calculated as the sum of the fluxes reaching that pixel, generated at each point on the catcher. This can be expressed mathematically as

$$N_{n,(x_d,y_d)} = \sum_{(x_c,y_c)} \sum_{E} Y_n(E, \theta'') \cdot N_{ion,(x_c,y_c)}(E)$$

where, $\theta'' = \tan^{-1}\left(\sqrt{(x_d - x_c)^2 + (y_d - y_c)^2}/L\right)$ and $L$ is the catcher-to-detector distance.

## 3. Results

Energetic ions of low atomic number, such as protons or deuterons, can be accelerated from laser-thin foil interaction via different acceleration mechanisms [8, 16, 17] depending on the laser and target parameters. However, TNSA has been so far the most studied and robust mechanism for ion acceleration at the currently available laser intensities, and has been used in most of the experiments studying neutron generation via pitcher-catcher scheme (see [6] and references therein). Therefore, we used a typical TNSA-type deuteron beam (divergent beam of exponential spectrum) in our code in order to study the effect of ion beam temperature and divergence on neutron beam divergence.

In order to study the beamed neutron emission observed in our experiment employing the petawatt arm of the VULCAN laser at Rutherford Appleton Laboratory (RAL), STFC, UK [6], we used the experimentally measured deuteron spectrum as the input to our model. The ion beams in the experiment were produced by irradiating 10 $\mu$m-thick deuterated plastic foils

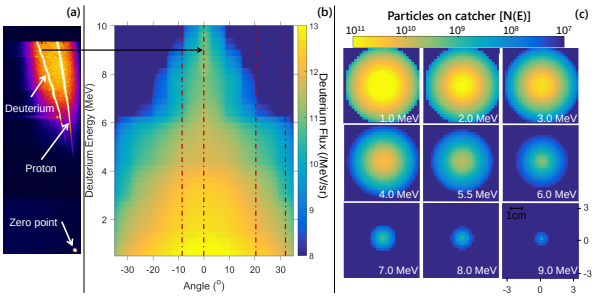


Figure 2: **(a)** A typical raw data obtained by a TPS diagnosing ion spectrum along the target normal direction. **(b)** Angularly resolved deuteron spectrum reconstructed from the data obtained by four TPS measurements along different angles (as shown by the dashed line) with respect to the target normal direction. **(c)** Spatial profiles of deuteron beam for different energies at the catcher plane.

at a peak intensity in excess of $10^{20}$ W cm$^{-2}$. The ion beam spectrum was diagnosed along different emission angles with respect to the target normal by employing Thomson Parabola Spectrometers(TPS). Due to the limitation of TPS in retrieving the spectrum of overlapping species, a differential filtering technique [18] was implemented to discriminate the deuterium ions from the overlapping species with equal charge-to-mass ratio, such as $C^{6+}$ and $O^{8+}$ originated from the target and hydrocarbon contaminant layers. A typical raw data obtained along the target normal direction is shown in Fig. 2(a). The deuteron spectra obtained from the different TPS were used to reconstruct the full beam profile, as shown in Fig. 2(b), while assuming an axis-symmetrical beam profile. The data shows a divergent ($\sim 60°$ full cone) beam of deuterons with an exponential spectrum, being the highest energies produced along the target normal direction with a narrow ($\sim 15°$) beam divergence, as expected from TNSA mechanism for such laser and target parameters.

The angularly resolved deuteron spectra shown in Fig. 2(c) was used in our code to simulate the neutron generation in the catcher placed at a distance of $l = 5$ mm from the ion source (which represents the point of laser interaction with the pitcher target). The flux distribution of the deuterons of different energies at the front surface of the catcher are shown in Fig. 2(c), which was obtained by using the beam profile shown in Fig. 2(b).

Despite of the moderate energies of the ions and the broad emission angle produced in the experiment, the simulation shows a directional beam-like emission of neutrons from the catcher target, as shown in Fig. 3 (showing neutron flux distribution across the detector plane placed at a distance $L = 15$ mm from the

catcher), with a Full Width at Half Maximum (FWHM) divergence of $\sim 60^\circ$ and maximum flux along the ion beam axis. The simulated neutron beam profile is similar to that obtained from the experiment (FWHM of $(70 \pm 10)^\circ$) as reported by Kar *et al.*. Since the simulated neutron beam profile was obtained by considering only the d(d,n)$^3$He reaction, the residual difference between the simulated and experimental neutron beam profile is most likely due to a range of additional nuclear reactions taking place in the catcher in the latter case. As discussed in Ref. [6], due to the higher flux and higher energy protons produced from the pitcher target (as can be seen in Fig. 2(a)), the proton-induced deuteron breakup reaction (d(p,n+p)$^1$H) contributes significantly towards the total neutron yield. Due to the reaction kinematics, this nuclear reaction is expected to produce a narrow neutron beam divergence, similar to that obtained for the d(d,n)$^3$He reaction. However, a detailed simulation for the d(p,n+p)$^1$H case could not be carried out due to the insufficient reaction cross-section available in the literature.

In order to study the effect of the projectile ion beam parameters on the neutron beam divergence, we carried out a set of simulations by varying the input spectrum of the ions, as expected to be produced by TNSA mechanism at different laser intensities. The ion temperature and the cut-off ion energy in the TNSA mechanism scale with the temperature of the hot electrons

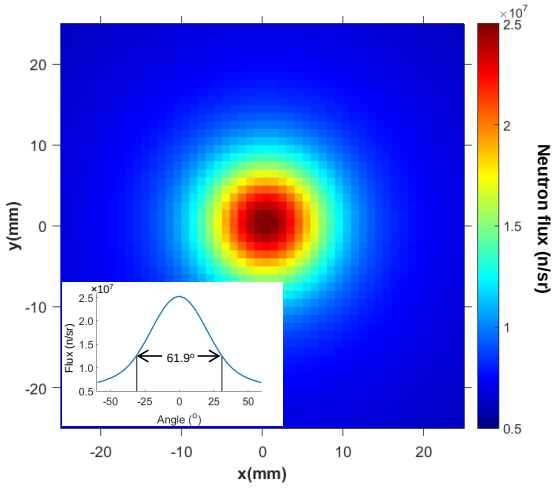


Figure 3: Simulated neutron beam reaching a flat detector in front of the catcher. Inset shows the lineout of the neutron beam profile across the detector, which also represents the emission angle of neutrons with respect to the ion beam axis. The divergence of the neutron beam (FWHM) is $\sim 60^\circ$.

produced by the interaction, which broadly scales as $\sqrt{I_L \lambda^2}$ [8, 19, 20, 21], where $I_L$ and $\lambda$ stand, respectively, for the intensity and the wavelength of the incident laser. The divergence of the ions produced by the TNSA mechanism also varies within the beam depending on its energy [22] - ions with higher energy are emitted with a lower divergence. Assuming a flat-top flux profile within the ion beam divergence, and the following divergence profile as a function of ion energy (as reported for ~ps lasers in Ref. [22]),

$$\theta_D(E, E_{max}) = \begin{cases} 62 & E < E_{max}/2 \\ 107.4 - 90.9 \cdot \frac{E}{E_{max}} & E \geq E_{max}/2 \end{cases}, \quad (1)$$

we modelled an input TNSA beam profile for our simulations as a function of laser intensity, as given by

$$\frac{d^2 N_{ion}}{dE\, d\Omega} = \frac{dN_{ion}}{dE}\bigg|_{\substack{E<E_{max} \\ \theta<\theta_D}} \propto \exp\left(-\frac{E}{k_B T(I_L)}\right) \quad (2)$$

A set of simulations were carried out by varying the ion beam temperature $k_B T(I_L)$. The cut-off energy for the deuterons as a function of laser intensities was assumed as $E_{max}(I_L) \sim 10^{-9} \sqrt{I_L}$ MeV, where the proportionality constant was calculated using the maximum deuteron energy obtained in our experiment, shown in Fig. 2(b).

The FWHM divergence of the neutron beam obtained from the simulations is shown in Fig. 4. One can see how the neutron beam divergence reduces significantly with an increase in the ion beam temperature. While a nearly isotropic emission for low ion temperatures is produced, the neutron beam divergence can be reduced below $50^\circ$ using higher power lasers than that used in our experiment. Intense lasers will produce ions at higher energies, which will provide two-fold enhancement to the on-axis neutron flux - (1) neutron yield per incident ion will increase significantly due to their deeper penetration into the catcher, (2) higher anisotropicity due to differential cross-section and kinematics (see Eq. 2 in Ref. [6]). An alternative approach for increasing the flux and energy of ions other than protons, which are preferentially accelerated by the TNSA mechanism, would be to use some special technique to eliminate the hydrogen contamination layer at the rear side of the pitcher target, such as depositing a layer of heavy water contamination for enhancing the deuteron acceleration [23].

The rate of decrease in neutron beam divergence slows down towards the higher temperatures, as visible in the Fig. 4. The nearly constant divergence of $\sim 30^\circ$ obtained for the high ion temperatures is due to the, albeit small, intrinsic divergence ($\sim 15^\circ$) of the highest

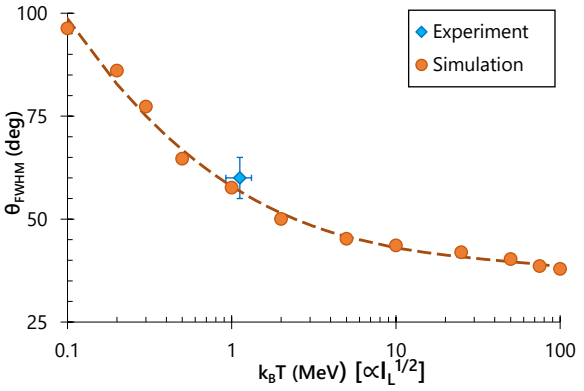


Figure 4: Neutron beam FWHM divergence as a function of the ion beam temperature obtained from our simulations. The blue data point shows the beam divergence obtained for the d(d,n)$^3$He reaction using the deuteron beam profile obtained from our experiment discussed above.

energy ions produced by the TNSA mechanism. This limitation in the neutron beam divergence can be easily eliminated by focussing the ion beams on the catcher, for example by using one of the several schemes reported in literature, such as permanent/pulsed magnetic focusing devices [24, 25, 26], laser-driven microlens[27], hemi-spherical targets [28], shaped targets [29] etc. Using a focussed beam of ions with narrow energy band can also help reducing the pulse duration of emitted fast neutrons, as recently reported by Higginson *et al.*[30].

## 4. Conclusions

We presented results obtained from a numerical model simulating the neutron beam generation by laser-driven ions in a pitcher-catcher scenario. Simulation results closely agree with the experimentally obtained neutron beam profile while using the experimentally measured ion beam profile in the simulation. By varying the ion beam parameters, simulations show an improvement in the neutron beam divergence with an increase in the ion beam temperature and cut-off energy, as expected from the TNSA mechanism at higher laser intensities.

## 5. Acknowledgements

The authors acknowledge funding from EPSRC [EP/J002550/1-Career Acceleration Fellowship held by S. K., EP/L002221/1, EP/K022415/1, EP/J500094/1. Authors acknowledge support of engineering, target fabrication and experimental science groups of Central Laser Facility of STFC, UK.

[1] L. Gray, J. Read, Treatment of cancer with fast neutrons, Nature 152 (1943) 53.

[2] A. Buffler, Contraband detection with fast neutrons, Radiation Physics and Chemistry 71 (3) (2004) 853–861.

[3] D. Vartsky, I. Mor, M. Goldberg, D. Bar, G. Feldman, V. Dangendorf, K. Tittelmeier, M. Weierganz, B. Bromberger, A. Breskin, Novel detectors for fast-neutron resonance radiography, Nuclear Instruments and Methods in Physics Research Section A: Accelerators, Spectrometers, Detectors and Associated Equipment 623 (1) (2010) 603–605.

[4] L. Perkins, B. Logan, M. Rosen, M. Perry, T. D. de la Rubia, N. Ghoniem, T. Ditmire, P. Springer, S. Wilks, The investigation of high intensity laser driven micro neutron sources for fusion materials research at high fluence, Nuclear Fusion 40 (1) (2000) 1.

[5] A. Wiedenmann, U. Keiderling, K. Habicht, M. Russina, R. Gähler, Dynamics of field-induced ordering in magnetic colloids studied by new time-resolved small-angle neutron-scattering techniques, Physical review letters 97 (5) (2006) 057202.

[6] S. Kar, A. Green, H. Ahmed, A. Alejo, A. Robinson, M. Cerchez, R. Clarke, D. Doria, S. Dorkings, J. Fernandez, et al., Beamed neutron emission driven by laser accelerated light ions, arXiv preprint arXiv:1507.04511.

[7] S. Atzeni, J. Meyer-ter Vehn, The Physics of Inertial Fusion: BeamPlasma Interaction, Hydrodynamics, Hot Dense Matter: BeamPlasma Interaction, Hydrodynamics, Hot Dense Matter, Vol. 125, Oxford University Press, 2004.

[8] A. Macchi, M. Borghesi, M. Passoni, Reviews of Modern Physics 85 (2013) 751.

[9] Extreme light infraestracture(eli) (`http://www.eli-np.ro/`).

[10] J. Zou, C. Le Blanc, D. Papadopoulos, G. Chériaux, P. Georges, G. Mennerat, F. Druon, L. Lecherbourg, A. Pellegrina, P. Ramirez, et al., Design and current progress of the apollon 10 pw project, High Power Laser Science and Engineering 3 (2015) e2.

[11] D. B. Pelowitz, et al., Mcnpx users manual version 2.5. 0, Los Alamos National Laboratory 76.

[12] J. Davis, G. Petrov, Angular distribution of neutrons from high-intensity laser–target interactions, Plasma Physics and Controlled Fusion 50 (6) (2008) 065016.

[13] D. Gwynne, S. Kar, D. Doria, H. Ahmed, M. Cerchez, J. Fernandez, R. Gray, J. Green, F. Hanton, D. MacLellan, P. McKenna, Z. Najmudin, D. Neely, J. Ruiz, A. Schiavi, M. Streeter, M. Swantusch, O. Willi, M. Zepf, M. Borghesi, Modified thomson spectrometer design for high energy, multi-species ion sources, Review of Scientific Instruments 85 (3). doi:10.1063/1.4866021.

[14] K. Lancaster, S. Karsch, H. Habara, F. Beg, E. Clark, R. Freeman, M. Key, J. King, R. Kodama, K. Krushelnick, et al., Characterization of 7li (p, n) 7be neutron yields from laser produced ion beams for fast neutron radiography, Physics of plasmas 11 (7) (2004) 3404–3408.

[15] G. Petrov, D. Higginson, J. Davis, T. B. Petrova, J. McNaney, C. McGuffey, B. Qiao, F. Beg, Generation of high-energy (¿ 15 mev) neutrons using short pulse high intensity lasers, Physics of Plasmas (1994-present) 19 (9) (2012) 093106.

[16] H. Daido, M. Nishiuchi, A. S. Pirozkhov, Report on Progress in Physics 75 (2012) 056401.

[17] M. Borghesi, J. Fuchs, S. Bulanov, A. Mackinnon, P. Patel, M. Roth, Fast ion generation by high-intensity laser irradiation

of solid targets and applications, Fusion Science and Technology 49 (3) (2006) 412–439.

[18] A. Alejo, S. Kar, H. Ahmed, A. Krygier, D. Doria, R. Clarke, J. Fernandez, R. Freeman, J. Fuchs, A. Green, J. Green, D. Jung, A. Kleinschmidt, C. Lewis, J. Morrison, Z. Najmudin, H. Nakamura, G. Nersisyan, P. Norreys, M. Notley, M. Oliver, M. Roth, J. Ruiz, L. Vassura, M. Zepf, M. Borghesi, Characterisation of deuterium spectra from laser driven multi-species sources by employing differentially filtered image plate detectors in thomson spectrometers, Review of Scientific Instruments 85 (9). doi:10.1063/1.4893780.

[19] P. Mora, Plasma expansion into a vacuum, Phys. Rev. Lett. 90 (2003) 185002. doi:10.1103/PhysRevLett.90.185002.
URL http://link.aps.org/doi/10.1103/PhysRevLett.90.185002

[20] J. Fuchs, P. Antici, E. dHumières, E. Lefebvre, M. Borghesi, E. Brambrink, C. Cecchetti, M. Kaluza, V. Malka, M. Manclossi, et al., Laser-driven proton scaling laws and new paths towards energy increase, Nature Physics 2 (1) (2005) 48–54.

[21] L. Robson, P. Simpson, R. Clarke, K. Ledingham, F. Lindau, O. Lundh, T. McCanny, P. Mora, D. Neely, C.-G. Wahlström, et al., Scaling of proton acceleration driven by petawatt-laser–plasma interactions, Nature Physics 3 (1) (2006) 58–62.

[22] F. Nürnberg, M. Schollmeier, E. Brambrink, A. Blažević, D. Carroll, K. Flippo, D. Gautier, M. Geißel, K. Harres, B. Hegelich, et al., Radiochromic film imaging spectroscopy of laser-accelerated proton beams, Review of scientific instruments 80 (3) (2009) 033301.

[23] A. Krygier, J. Morrison, S. Kar, H. Ahmed, A. Alejo, R. Clarke, J. Fuchs, A. Green, D. Jung, A. Kleinschmidt, et al., Selective deuterium ion acceleration using the vulcan petawatt laser, Physics of Plasmas (1994-present) 22 (5) (2015) 053102.

[24] M. Schollmeier, S. Becker, M. Geißel, K. Flippo, A. Blažević, S. Gaillard, D. Gautier, F. Grüner, K. Harres, M. Kimmel, et al., Controlled transport and focusing of laser-accelerated protons with miniature magnetic devices, Physical review letters 101 (5) (2008) 055004.

[25] M. Nishiuchi, I. Daito, M. Ikegami, H. Daido, M. Mori, S. Orimo, K. Ogura, A. Sagisaka, A. Yogo, A. Pirozhkov, et al., Focusing and spectral enhancement of a repetition-rated, laser-driven, divergent multi-mev proton beam using permanent quadrupole magnets, Applied Physics Letters 94 (6) (2009) 061107.

[26] S. Ter-Avetisyan, M. Schnürer, R. Polster, P. Nickles, W. Sandner, First demonstration of collimation and monochromatisation of a laser accelerated proton burst, Laser and Particle Beams 26 (04) (2008) 637–642.

[27] T. Toncian, M. Borghesi, J. Fuchs, E. d'Humières, P. Antici, P. Audebert, E. Brambrink, C. A. Cecchetti, A. Pipahl, L. Romagnani, et al., Ultrafast laser-driven microlens to focus and energy-select mega-electron volt protons, Science 312 (5772) (2006) 410–413.

[28] S. Kar, K. Markey, M. Borghesi, D. Carroll, P. McKenna, D. Neely, M. Quinn, M. Zepf, Ballistic focusing of polyenergetic protons driven by petawatt laser pulses, Physical review letters 106 (22) (2011) 225003.

[29] S. Kar, K. Markey, P. Simpson, C. Bellei, J. Green, S. Nagel, S. Kneip, D. Carroll, B. Dromey, L. Willingale, et al., Dynamic control of laser-produced proton beams, Physical review letters 100 (10) (2008) 105004.

[30] D. Higginson, L. Vassura, M. Gugiu, P. Antici, M. Borghesi, S. Brauckmann, C. Diouf, A. Green, L. Palumbo, H. Petrascu, et al., Temporal narrowing of neutrons produced by high-intensity short-pulse lasers, Physical review letters 115 (5) (2015) 054802.